Chapter 2

Instrumentation for Ferromagnetic Resonance Spectrometer

Chi-Kuen Lo

Additional information is available at the end of the chapter

http://dx.doi.org/10.5772/56069

1. Introduction

Even FMR is an antique technique, it is still regarded as a powerful probe for one of the modern sciences, the spintronics. Since materials used for spintronics are either ferromagnetic or spin correlated, and FMR is not only employed to study their magneto static behaviors, for instances, anisotropies [1,2], exchange coupling [3,4,5,6], but also the spin dynamics; such as the damping constant [7,8,9], g factor [8,9], spin relaxation [9], etc. In this chapter a brief description about the key components and techniques of FMR will be given. For those who have already owned a commercial FMR spectrometer could find very helpful and detail information of their system from the instruction and operation manuals. The purpose of this text is for the one who want to understand a little more detail about commercial system, and for researchers who want to build their own spectrometers based on vector network analyzer (VNA) would gain useful information as well.

FMR spectrometer is a tool to record electromagnetic (EM) wave absorbed by sample of interest under the influence of external DC or Quasi DC magnetic field. Simply speaking, the spectrometer should consist of at least an EM wave excitation source, detector, and transmission line which bridges sample and EM source. The precession frequency of ferromagnetics lies at the regime of microwave (μ-wave) ranged from 0.1 to about 100 GHz, therefore, FMR absorption occurs at μ-wave range. The generation, detection and transmission at such this high frequency are not as simple as those for DC or low frequency electronics. According to transmission line and network theories [10,11], impedance of 50 Ω between transmission line and load has to be matched for optimization of energy transfer. FMR spectrometer also has a resonator and an electro magnet which produces magnetic field to vary the sample's magnetization during the measurement. Sample which is mounted inside the cavity absorbs energy from the μ-wave source. The detector electronics records the changes on either the reflectance or transmittance of theμ -wave while magnetic

field is being swept [12]. Most commercial spectrometers, for examples, ELEXSYS-II E580, Bruker Co [13], and JES-FA100, JOEL Ltd. [14], character FMR by measuring the reflectance at fixed band frequency. μ-wave is generated by a Klystron, which goes to a metallic cavity via a wave guide. Signal reflected back from the cavity through the same waveguide to a detector, the Schottky barrier diode. Noted that a circulator is employed, such that the μ-wave does go to the detector and not return back to the generator. The integration of the source, detector, circulator, protected electronics, etc. in a single box, is named "Microwave Bridge". The basic configuration of most FMR spectrometer is shown in Fig.1. FMR absorption spectrum is obtained by comparing the incident and reflected signals. However, the signal to noise ratio (SNR) given by this kind of reflectometer is still not large enough to recognize the spectrum, and lock-in technique is needed to enhance SNR to acceptable value, for example, bigger than 5.

The operational frequency of the source, detector and cavity cannot be varied broadly, therefore, it is necessary to change the microwave bridge and cavity while working with different band frequency. Dart a glance at a FMR spectrometer, the key parts are the microwave bridge, cavity, gauss meter, electromagnet, and lock-in amplifier for signal process. Surely, automation and data acquisition are also crucial.

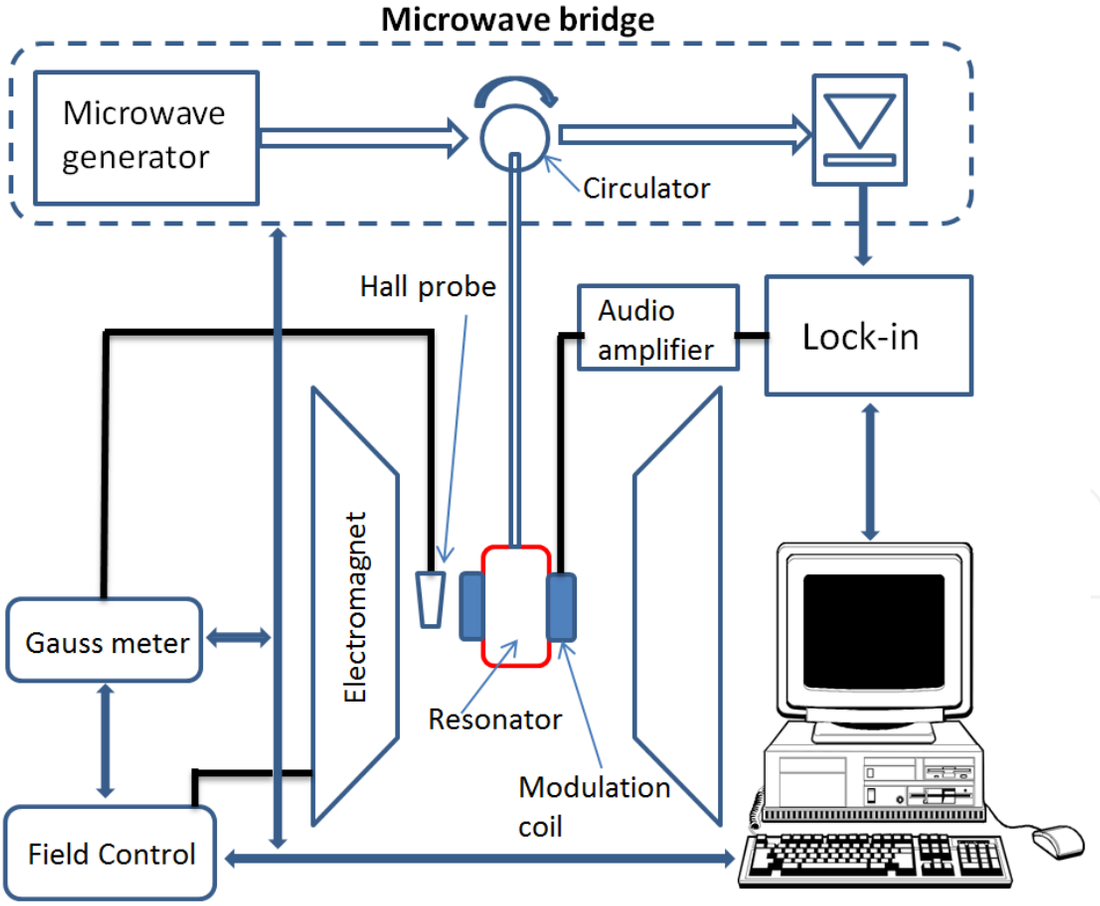

Figure 1. Basic configuration of FMR spectrometer. The microwave bridge mainly consists of the microwave generator, circulator, and detector.

2. Key components of FMR

2.1. Metallic cavity

A Metallic resonator (cavity) is a space enclosed by metallic walls which sustain electromagnetic standing wave or electromagnetic oscillation. The cavity has to be coupled with external circuit which provides excitation energy. On the other hand, the excited cavity supplies energy to the sample of interest (loading) through coupling [10,11]. The basic structure of a cavity set is sketched as in Fig.2(a), which consists of a wave guide, a coupler with iris control, and a metallic cavity. The working principle of coupled cavity can be understood by using LRC equivalent circuit which couples to a transmission line [10,11] as shown in Fig.2(b) and 2(c). The coupling structure is represented by an ideal transformer with transforming ratio 1:n. The parallel RLC circuit could be transformed to T_s from AB plane via the transformer, such that $C'=n^2C$, $R'=R/n^2$, and $L'=L/n^2$. The resonance frequency, f_{res}, and Q-factor will not be affected by the transformation [10] as pointed out by eq.(1) and eq.(2), respectively:

$$\omega_0' = \frac{1}{\sqrt{L'C'}} = \frac{1}{\sqrt{\frac{L}{n^2}n^2C}} = \omega_0 \tag{1}$$

$$Q_0' = \omega_0' C' R' = \omega_0 n^2 C \frac{R}{n^2} = \omega_0 CR = Q_0 \tag{2}$$

A coupling coefficient, β, which defines the relation between energy dissipation (E_d) in a cavity and energy dissipation of external circuit (E_e), tells if the cavity is coupled with external circuit.

$$\beta \equiv \frac{E_d}{E_e} = \frac{\frac{U^2}{2Z_C}}{\frac{U^2}{2R/n^2}} = \frac{R}{Z_C n^2} = \frac{R'}{Z_C} \tag{3}$$

U in eq.(3) stands for the voltage applied to the cavity, and 1:n is the transforming ratio for tuning to critical couple state ($Z_C = R' \Rightarrow \beta = 1$) before doing FMR measurement. The characterization impedance, Z_C, is always designed to be 50Ω (Z_0) for matching impedance as mentioned previously. Signal will be distorted and weakened if working at either under-coupling (β<1) or over-coupling states (β>1). The external Q factor (Q_e) of a cavity, coupled to external circuit, states the energy dissipation in the external circuit, and also has the following relationship with β:

$$\beta = \frac{Q_0}{Q_e} \tag{4}$$

In eq.(4), Q_0 is the intrinsic Q factor of cavity. Practically, the loaded Q-factor, Q_L, is used in experiments:

$$Q_L = Q_0 \frac{\beta}{1+\beta}\ ; \text{or } \frac{1}{Q_L} = \frac{1}{Q_0} + \frac{1}{Q_e} \tag{5}$$

Metallic cavities used for FMR measurement have to be TE mode, such that the cavity center which is also the sample location has maximum excitation magnetic field. Furthermore, this kind of cavity has very high Q-factor and plays key role in FMR detection. The signal output, V_S, from the cavity can be expressed as [15]:

$$V_S = \chi"\eta Q_L \sqrt{PZ_0} \tag{6}$$

χ",η , P and Z_0 in eq.(6) stand for imaginary part of magnetic susceptibility of the sample, filling factor, microwave power, and characteristic impedance, respectively. The Q-factor of a cavity directly relates to the detecting sensitivity, which depends very much on the design and manufacturing technique. A good metallic cavity normally has unloaded Q-factor of more than 5,000 which cannot be changed after being manufactured, and therefore is regarded as a constant in eq.(6). Z_0 of 50Ω is fixed for matching the network impedance. We cannot play too much on χ" and η as well, since the former is the intrinsic behaviour of the sample of interest to be tested, and the last parameter is the volume ratio of the sample and cavity. For thin film and multilayer samples, η is very small, hence this term cannot contribute too much to V_S. The source power, P, at the first glance, is the only possible adjustable parameter for sensitivity. Due to the occurrence of saturation, higher power may not be that helpful in increasing the FMR signal. Large excitation power drives magnetization precession in non-linear region which complicates the spectrum analysis. Besides, signal will be reduced and broadened while operating at saturation region. In order to determine the line shapes and widths precisely, this region should be avoided, hence low power is a good choice. The determination of saturation power is not difficult, since the signal intensity grows as the square root of power as indicated by eq.(6). Checking the signal intensity to see if eq.(6) is still validated as the power is increased. It is noted that the maximum excitation power of a common VNA is just a few mWs, and V_S is not that clear to follow √P.

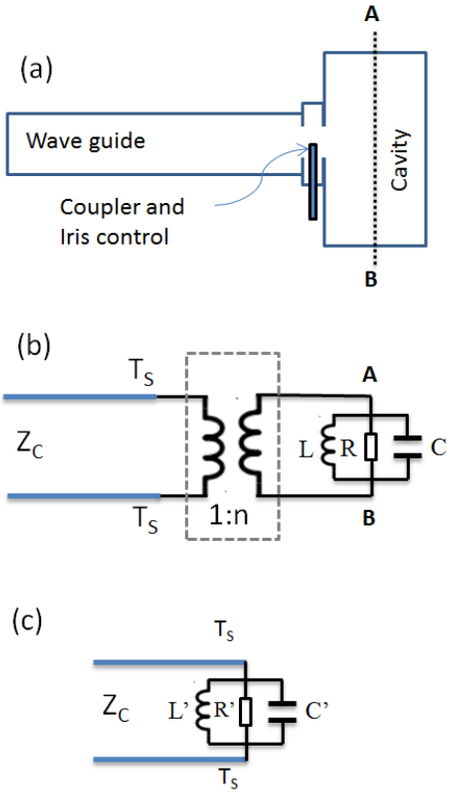

Figure 2. (a) The layout of a resonant cavity, (b) The equivalent LRC circuit. The iris control is regarded as a transformer, and (c) The equivalent circuit transformed to the T_S plane [10].

The Q-factor of commercial or home-made cavities can be determined easily by using a VNA, which can also be expressed as:

$$Q = \frac{f_{res}}{\Delta f} \tag{7}$$

f_{res} is the resonant frequency of a cavity, and Δf, is the full width at half maximum (FWHM) of the resonant peak. Eq.(7) can be simply found by a built-in function of VNA which measures directly the reflected power of the cavity in dB at f_{res}. Besides with dB unit, FWHM (Δf) is also obtained at half power point, i.e. the power level at -3dB. As the values of f_{res} and FWHM are known, Q is determined as shown in Fig.3(d).

Q will be decreased once a sample is inserted. This is because the inserted sample and its holder absorb energy and change the coupling conditions resulting in Q reduction and resonance frequency shift. However, these deviations can be amended a little bit by adjusting the iris which controls the effective impedance by varying the aperture size between the cavity and wave guide, and by adjusting the position of metallic cap. This is equivalent to change the transformer ratio, that is, the equivalent inductance and capacitance. The iris control is a plastic screw (low μ-wave absorption material) which has a gold coated metal cap on one end, and the effective impedance of the whole (wave guide + iris + cavity) depends on the size of the aperture and location of the metal cap. The function of the iris acts as a device to tune the L and C, such that the cavity is critical couple again. As field is swept, the variations of sample's magnetization break the coupling condition so the cavity is deviated from critically coupled state. Consequently, wave is reflected back to the ◎-wave bridge, and FMR signal is resulted.

For an ideal metallic cavity (infinite conductivity and perfectly smooth inside wall surface), there will be a unique resonant peak with infinite large Q-factor, However, this is not the case in practice. Since the cavity itself has finite conductivity, and further, the inside wall is not perfectly flat, these cause the existence of many peaks with very low Q values as extracted by a VNA shown in Fig.3(a). Fig.3(b) shows the simulation of a copper made cavity with a very rough inside wall. As the roughness is reduced, the spectrum is clearer as shown in Fig. 3(c). This could be due to the μ-wave which is multi-scattered by lumps on the wall surface, and these lumps could also enhance power dissipation further. In consequence, there exists many low Q peaks. Even there are many peaks other than the eigen frequency, these peaks do not response to the change of magnetization, and hence useless for FMR characterization. The manufacture of metallic cavity with Q-factor of higher than 3,000 is laboring. This is because the inside wall has to be mirror polished and coated with a few μm thick Au layer to reduce the imperfection.

Fig.3(a) and Fig.3(d) are the frequency response of a Bruker X-band cavity (TE_{102}, ER 4104OR) exhibiting in larger and smaller frequency windows, respectively. The unloaded Q-factor of this cavity is ~9,000 as claimed by the manufacturer, however, our measurement tells that the Q factor is more than 14,000. This is because frequency resolution of the VNA is very high. As the resolution is decreased, Q is found to be decreased as well.

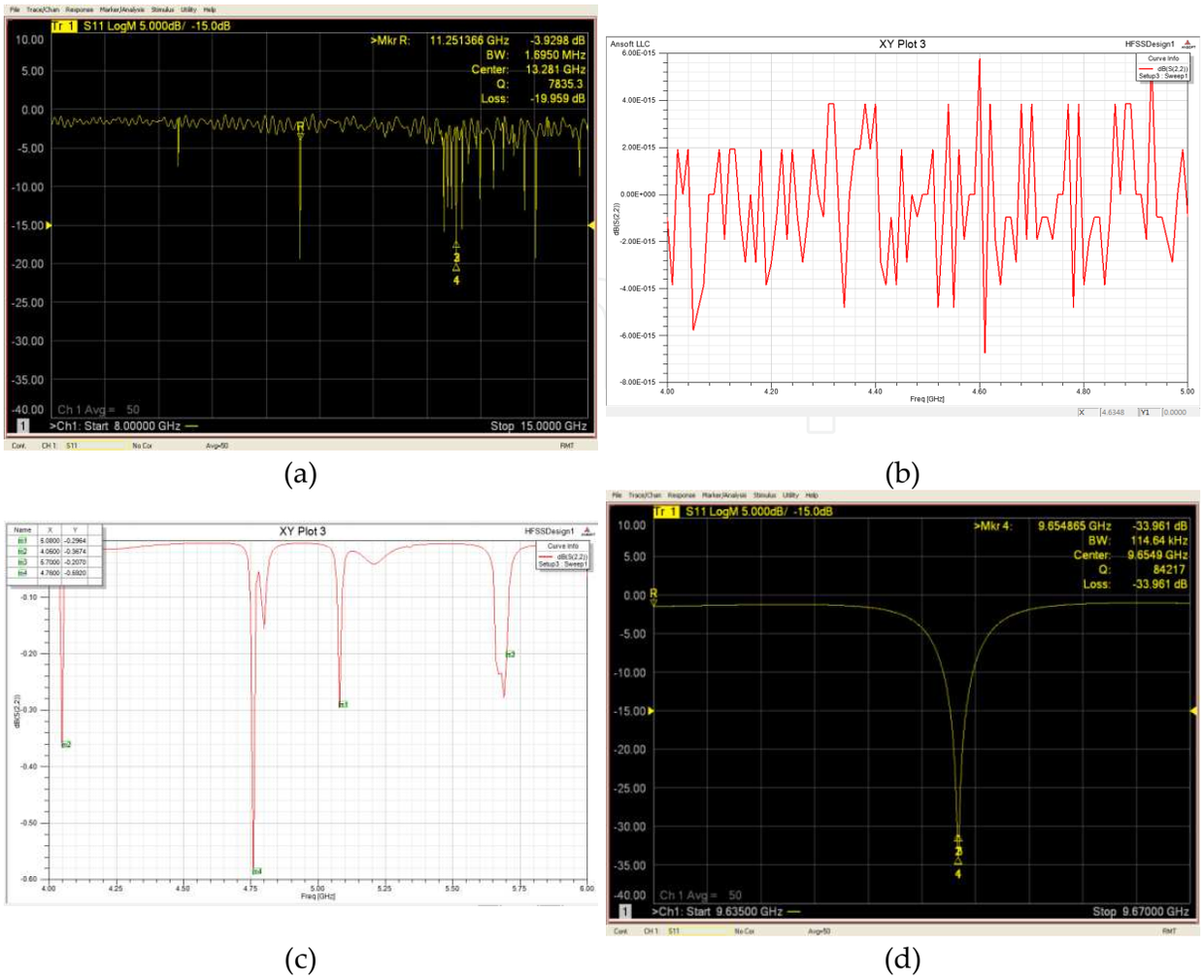

Figure 3. (a) the frequency response of a X-band cavity. Simulation result of a Cu cavity with (b) a very rough inside wall surface, and (c) a smooth inside wall surface. (d) VNA measurement of an X-band cavity with Q higher than 87, 000. Note that there are many side peaks but not appears in this frequency range

2.2. Shorted waveguide cavity

The fabrication of metallic cavity with very high Q-factor is not easy as mentioned above. If the lossy of the sample is not very big, cavity with Q of a few hundred to thousand may be good enough to recognize FMR. If so, a shorted waveguide cavity (SWC) could be an alternative. This kind of cavity is just a section of waveguide sealed by a metal plate at one end [16] as show in Fig.4. Since metallic wave guide are commercially standard with wide range of frequency from L to W band, it is worth to obtain FMR information at different bands with this cheap, simple and effective method. If the length of the waveguide tube is equal to $n\lambda/2$, standing wave can be formed inside. In that n and λ represents for integer and wave length of the μ-wave, respectively. In order to excite FMR signal, sample has to be placed at the $n\lambda/4$ position away from the shorted plate at which maximum magnetic field is located. In Fig.4, n=0 and n=1 are the suitable locations, however, n =0 gives advantages of easier sample manipulation, and lesser interference from irrelevant insertions. Sample is

mounted at the top of a plastic screw through the shorted plate, such that its position can be adjusted for maximum signal. However, SWC does not have an iris to tune the impedance, hence critical coupling may not be easy to obtain. Although the Q is somewhat lower (less than 2,000), SWC is easy to make from commercial waveguide tube. Furthermore, different band frequency cavity can be built in the same manner, and this is particular convenient to study FMR at different band frequency with network analyzer.

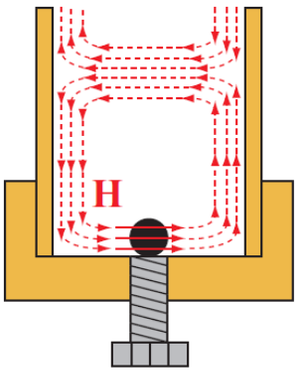

Figure 4. A shorted wave guide with possibility of sample manipulation. Magnetic field distribution originated from the μ-wave is also sketched [16].

2.3. Microstrip and co-planar waveguide

Microstrip (MS) and co-planar waveguide (CPW) which are indeed transmission lines, are commonly used to extract FMR at broad frequency range [16,17,18,19]. Sample is mounted on top of their signal lines, and μ-wave is conducted into MS (CPW) via Port 1 of the VNA, and the differential change in either reflected or transmitted signal is analyzed. In this operation scheme, frequency is swept at fixed field, and once the FMR conditions are fulfilled μ-wave absorption occurs. Fig.5 and Fig.6 are the sketches of MS and CPW. Since h << λ, μ-wave propagates in these two lines is regarded as quasi-TEM mode. In order to match the impedance of 50Ω, the dimensions of these two planar transmission lines are restricted.

In case of MS, we have the followings [11]:

The effective dielectric constant, ε_{eff} has approximately the form:

$$\varepsilon_{eff} = \frac{\varepsilon_r+1}{2} + \frac{\varepsilon_r-1}{2}\frac{1}{\sqrt{1+12h/w}} \tag{8}$$

The dimension of the strip line and characteristic impedance, Z_C, can be worked out as below:

$$Z_C = \begin{cases} \frac{60}{\sqrt{\varepsilon_{eff}}} ln\left(\frac{8h}{w}+\frac{w}{4h}\right) & ; \text{ for } w/d \le 1 \\ \frac{120\pi}{\sqrt{\varepsilon_{eff}\left[\frac{w}{d}+1.393+0.667\ ln\left(\frac{w}{d}+1.444\right)\right]}} & ; \text{ for } w/d \ge 1 \end{cases} \tag{9}$$

In case of CPW if the thickness of signal line is ignorable, then [10]:

$$\varepsilon_{eff} = \frac{\varepsilon_r + 1}{2} \tag{10}$$

$$Z_C = \begin{cases} \frac{\eta_0}{\pi\sqrt{\varepsilon_{eff}}} ln\left(2\sqrt{\frac{b}{w}}\right)\ \Omega & ;\ 0 < w/\mathrm{b} < 0.173 \\ \frac{\pi\,\eta_0}{4\sqrt{\varepsilon_{eff}}}\left[ln\left(2\frac{1+\sqrt{w/b}}{1-\sqrt{w/b}}\right)\right]^{-1}\ \Omega & ;\ 0.173 < \frac{\mathrm{w}}{\mathrm{b}} < 1 \end{cases} \tag{11}$$

η_0 in eq.(11) stands for the wave impedance in free space. The $Z_C = Z_0$ is set to 50Ω , then b, d and w can easily be determined from eq.(9) and eq.(11). The line width of the strip can be ranged from sub-millimeter to millimeters depending on the design and dielectric material used as implied by these equations. The size of this kind of line width can be fabricated simply by photo lithography together with life-off process. Due to the large loss, the characterization of nano size sample may not be easy and lock-in technique is needed for SNR enhancement as described in next section.

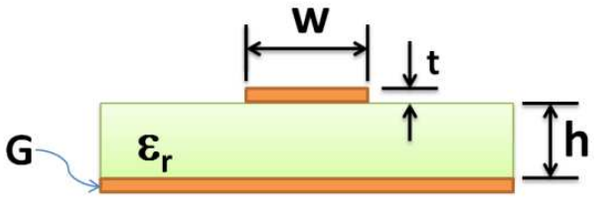

Figure 5. The geometry of a microstrip line, where εr is the relative dielectric constant of the substrate.

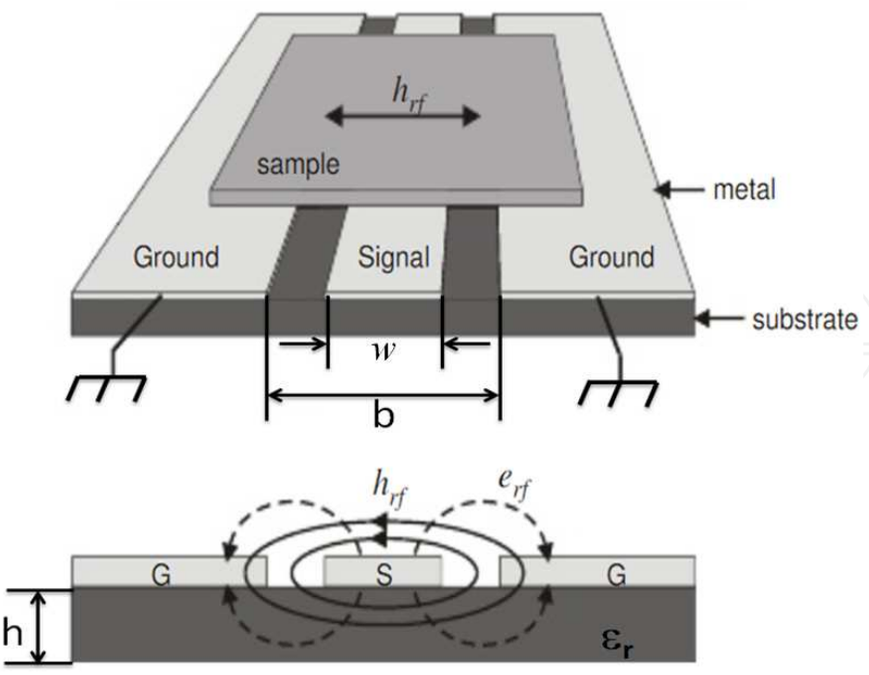

Figure 6. Schematical diagram of a coplanar waveguide along with the dimension. The lower diagram shows the magnetic (full lines) and electric (dashed lines) field lines winding around the signal conductor (S).

FMR can determined by characterizing the transmittance, ie. S_{12}. However, if shorted MS, and CPW are used, S_{11}, the reflectance FMR can also be found. Fig.7 shows the FMR of permalloy films extracted by VNA and CPW [18].

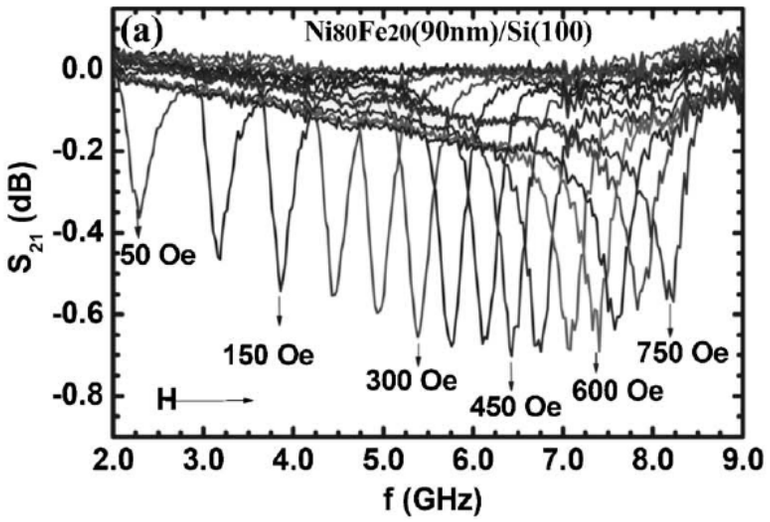

Figure 7. A typical FMR transmittance spectrum of permalloy films extracted by VNA with CPW [18].

3. Technique for signal to noise enhancement

3.1. Lock-in phase detection

If signal is deeply buried inside noise floor, lock-in method is normally employed to enhance the signal to noise ratio (SNR) by narrowing the detecting band window [20]. Considering a DC Signal, S, which is heavily contaminated by white noise, n, and for every measurement comes out from a measurement equipment, a voltmeter for an example, the reading can be expressed as:

$$\mathrm{V} = \mathrm{S} + n \tag{12}$$

If S can be modulated sinusoidally at a certain frequency somehow, then:

$$\mathrm{V}(t) = \mathrm{S}\cos(\omega t) + n \tag{13}$$

Note in eq.(13) that the modulation of white noise is still a white noise.

There is also a reference signal with same frequency but could be different in modulating amplitude (V_a) and phase (ϕ), i.e.,

$$V_{ref} = \mathrm{V}_a \cos(\omega t + \phi) \tag{14}$$

The product of eq.(13) and (14) gives:

$$\begin{aligned} \mathrm{V(t)}V_{ref} &= \mathrm{SV}_a \cos(\omega t)\cos(\omega t + \phi) + n\mathrm{V}_a \cos(\omega t + \phi) = \\ &\frac{\mathrm{SV}_a}{2}[\cos(\phi) + \cos(2\omega t + \phi)] + n\,V_a \cos(\omega t + \phi) \end{aligned} \tag{15}$$

The second and third terms can be eliminated if these two parts are passed to a low pass filter with cutoff frequency setting at ω/2 or lower. Finally, we have:

$$V \propto \frac{SV_a}{2}\cos(\phi) \tag{16}$$

That is, the signal is amplified by V_a, and has a maximum while ϕ is "phase-locked" to zero, hence the name of lock-in amplifier.

3.2. Feld modulation lock-in technique and derivative spectrum

It is easier to determine H_{res}, and ΔH_{pp} by differentiating the original signal. To do so, field modulation lock-in detection is employed and described below.

There is a small field, H_a, with modulation frequency of ω superposing on top of external DC magnetic field, H_0:

$$H(t) = H_0 + H_a\cos(\omega t) \tag{17}$$

Assuming we have FMR signal, V_{FMR}, whose Taylor expansion at H_0 is given below:

$$V_{FMR}(H) = V_{FMR}(H_0) + \left.\frac{dV_{FMR}}{dH}\right|_{H=H_0} H_a\cos(\omega t) + \cdots \tag{18}$$

Meanwhile, we also have another signal, the reference, which has the same frequency as that of the modulation field, but with a phase angle, ϕ:

$$V_{ref} = \cos(\omega t + \phi) \tag{19}$$

The product of eq.(18) and (19) gives eq.(20) below:

$$V_{FMR}(H) \times V_{ref} = V_{FMR}(H_0)\cos(\omega t + \phi)\left.\frac{dV_{FMR}}{dH}\right|_{H=H_0} + H_a\cos(\omega t)\cos(\omega t + \phi) + \cdots =$$
$$V_{FMR}(H_0)\cos(\omega t + \phi) + \frac{1}{2}\frac{dV_{FMR}}{dH}H_a\cos(\phi) + \frac{1}{2}\frac{dV_{FMR}}{dH}H_a\cos(2\omega t + \phi) + \cdots \tag{20}$$

The first and third terms in eq.(20) can again be removed by using a low pass filter with cutoff frequency setting at ω/2 or even lower. The second term is time independent, proportional to derivative of the input signal and magnify by H_a, which has a maximum if the phase, ϕ, is locked to 0. Another advantage of use this method is that 1/f noise and drift problem can be excluded by setting the sampling window at high frequency.

The way to turn the DC or quasi DC signal from to AC is an important subject. The simple and normal way to do this is to insert two coils which sandwich the cavity. These coils are driven by a power amplify at certain high frequency, such that an AC magnetic field of a few mT at a frequency up to 200 kHz can be produced. Therefore, the output signal consists of the modulation and DC components. All these together with the reference are sent to the lock-in amplify for SNR enhancement and derivative spectrum as mentioned previously. Modulation amplitude (MA), modulation frequency (MF), and time constant (TC) which is the reciprocal of the low pass filter's cutoff frequency, have large influence on the spectra.

Signal strength is linearly proportional to the MA while MA is small. Simply speaking, MA should be small enough for sampling in linear region, but needs to be large enough for gaining good sensitivity. However, too large the MA results in signal distortion as shown in Fig.8(a). This can be understood from eq.(20) that high order term cannot be ignored for large MA which causes distortion of derivative signal. The choice of MF is critical as well that small MF cannot get rid of 1/f noise completely, and elongates the acquisition time. Large MA and MF also cause passage effect that the rate of "passage" through the absorption line is faster than the relaxation rates, which results in distorted spectrum, or even inversion of signals upon reversal of the field scan direction. Therefore, it is important to check the FMR signal with either a standard or a well-known sample with different lock-in conditions for the best settings. In order to obtain correct line shape spectrum, the rule of thumb is to set the MA about 1/10 of the FWHM and increases to about 1/3 if necessary. TC also needs to coordinate with MF. According to Nyquist sampling theorem, the sampling rate should be at least twice the highest frequency contained in the signal [21]. For example, if the MF is 100 kHz, the sampling frequency would be at least 200 kHz at which TC is about 5μS. If this restriction does not fulfill, sampling points cannot not be captured immediately. Consequently, information loss and line shape distortion are always resulted. The best way to avoid this is to set the scan time for a FMR signal 10 times longer than the time constant.

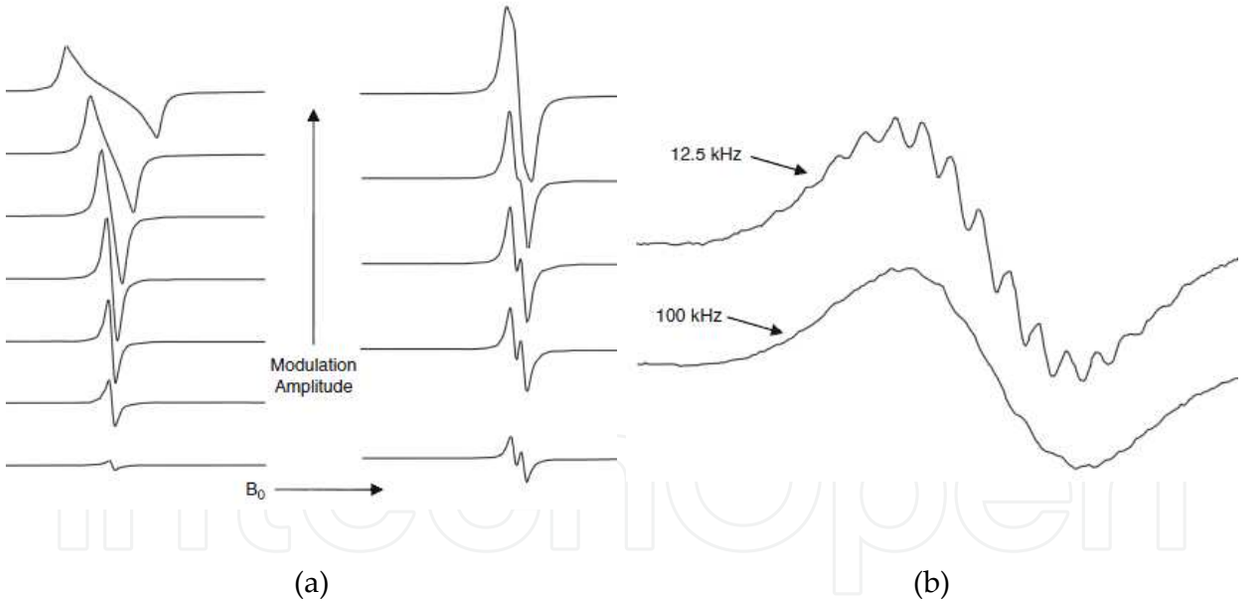

Figure 8. The influence of modulation amplitude (a) and modulation frequency (b) on signal. Distortion will be resulted if MA and MF are not appropriate [15].

4. Vector analyzer based FMR spectrometer

4.1. Basics of vector network analyzer (VNA)

VNA is indeed an instrument developed for characterization of electrical devices (device under test, DUT) by sending an electromagnetic wave. As an analogue of that in optics, the

incident wave (either optical or micro wave) will be reflected or/and transmit after interacting with the DUT. By examining the reflectance and transmittance, that is, the ratios of the powers of reflected, transmitted to that of the incident waves, scattering parameters of the DUT can be found as depicted in Fig.9. VNA cannot only find out the reflectance and transmittance, but also the impedance, phase lag, insertion loss, return loss, voltage standing ratio, etc., can be worked out. However for FMR experiment, only the first two functions are employed. VNA has at least two ports, and each port can produce and measure μ-wave. The scattering parameter S_{ij} stands for scattering power ratio of incident wave produced by port i, and measured by port j. That is, for a two-port VNA, S_{11} and S_{22} characterize wave reflectance, while S_{12} and S_{21} determine the transmittance. If FMR is determined by reflected spectrum, one port is enough by analyzing either the S11 or S22. For transmittance spectrum, two ports are required for either the S_{12}, or S_{21} determination. VNA has capability of microwave generation and detection, and furthermore, nowadays model has frequency ranged from about 0.1 to 100 GHz, or even higher at excitation power of tens dBm, Thus, it can serve as a microwave bridge to extract FMR parameters at a very broad frequency band. VNA measures not only the scattering amplitudes, but also their correlated phases. This is in contrast to its counterpart, the scalar network analyzer (SNA) which cannot tell phase information. FMR signal is extracted from power absorption which contains no phase information, and SNA should be good enough for the purpose. However, this kind of machine has been obsoleted for many years.

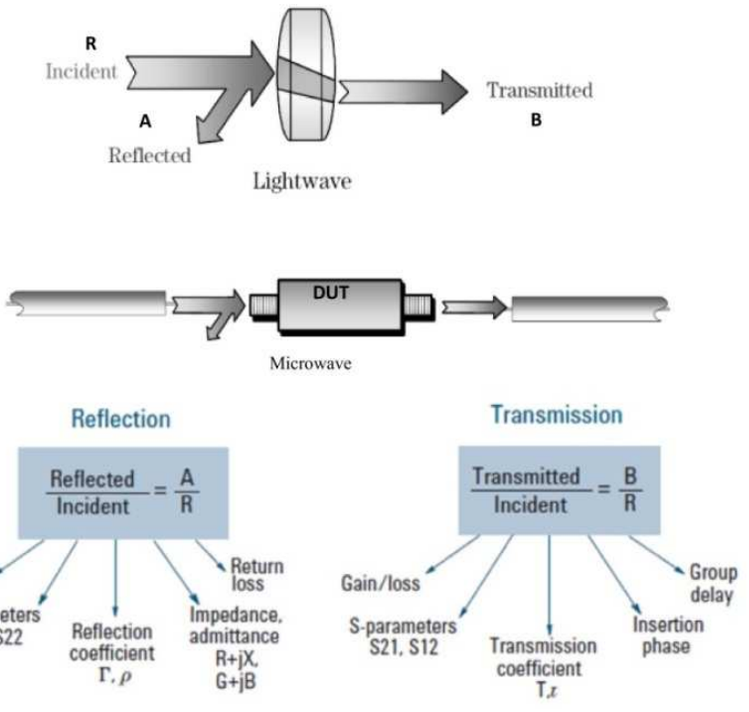

Figure 9. The fundamentals of microwave network analysis are analogue to that of the optics. The lower part of the panel indicates the definitions of scattering parameters [24].

VNA is commonly used with MS and CPW for FMR determination with frequency swept at fixed field. Since signal output from VNA cannot be plugged into lock-in amplifier directly,

the characterization of nano scale sample is thus difficult without using lock-in. The application lock-in with VNA will be discussed in next section.

4.2. Field swept VNA-FMR

Metallic cavity usually has rather higher Q-factor and could be simply used with a VNA for field swept FMR detection. Taking the advantages of high Q cavity and VNA, C.K. Lo, *et. al*. [23] demonstrated FMR measurement without employing field modulation lock-in technique. They employed a TE_{102} cavity with unload Q of ~9,000 at X-band, and FMR signal was recorded through the measurement of reflectance, and therefore one VNA port for S_{11} was used. This powerful method extracts signal easily and directly as shown in Fig.10(a). One could if necessary, differentiate the original data for derivative spectrum which is used to determine the peak position and line wide as those in commercial FMR spectrometer. Further, this combination has quite good sensitivity that 1.6 nm CoFeB can be detected with SNR better than 5 as shown in Fig.10(b).

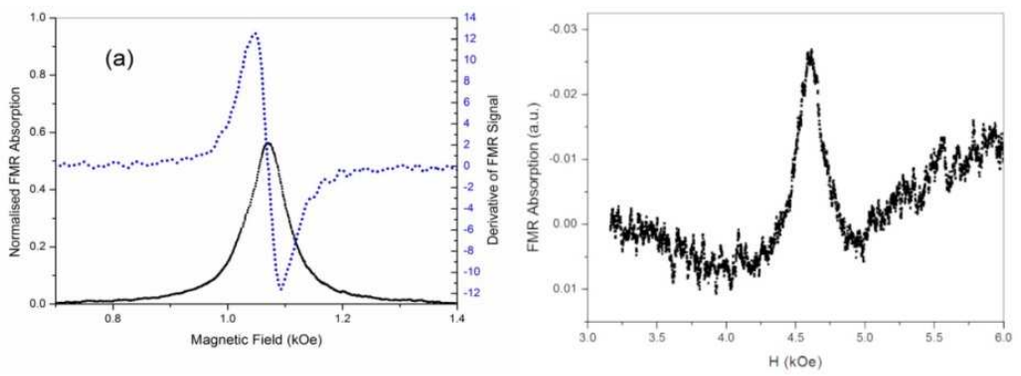

(a) (b)

Figure 10. (a) FMR of 5 nm Py exacted at P = 10 dBm. The dotted line is the derivative of experimental data. (b) Signal extracted from a 1.6nm CoFeB

A new built spectrometer should be characterized before properly used and well known samples, such as permalloy, Fe, Co, etc., ferromagnetics are normally employed due to their ΔH and peak positions can be found widely in literatures. Also, these samples are easy to prepare with different thicknesses, and results should be comparable to those in literatures reported.

There are many build-in useful functions with nowadays VNA, and only some of them are used, for instances, the traces of valley (dip) position, Q factor, band width, average, etc. Dip frequency and Q-factor will be varied as the sample's magnetization state is changed by external field. The changes of these quantities were also recorded simultaneously for a Fe/Ag multilayer as shown in Fig.11 in which (a) is the FMR absorption, and (b), the post derivative of (a). The shifts of resonant frequency and Q-factor are shown in (c) and (d), respectively. Despite the variation of center frequency is just a few hundreds MHz, it allows us to determine ferromagnetic parameters precisely. The change of Q-factor is upside-down to that of the absorption. This is because any absorption of microwave inside the cavity will reduce the Q value.

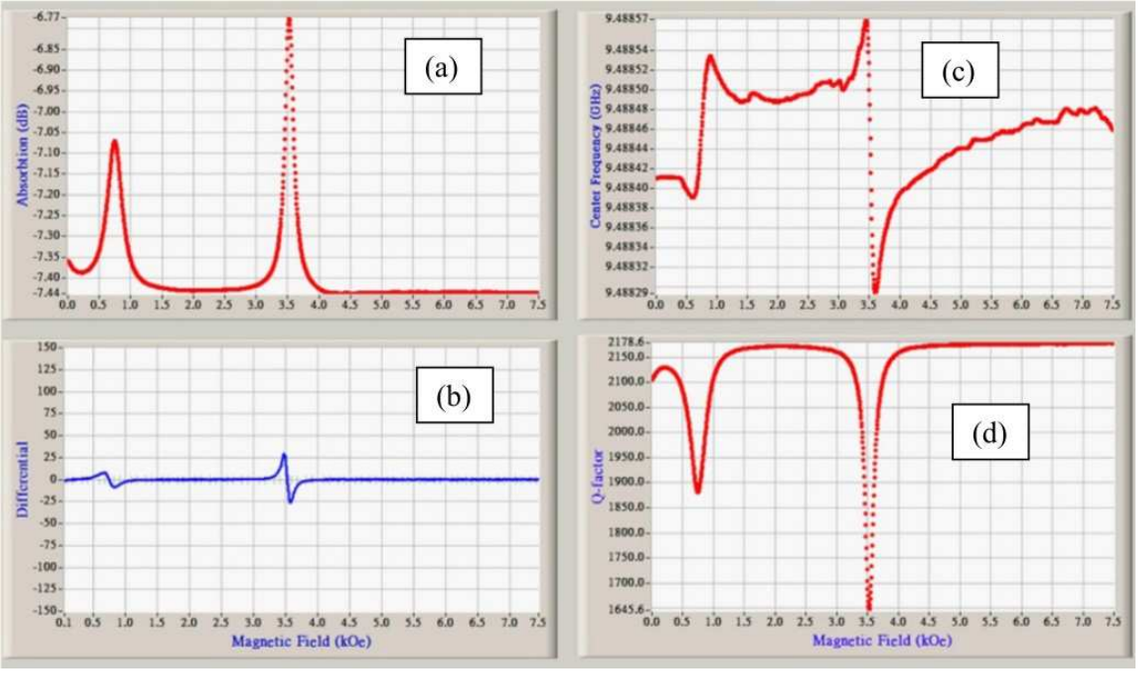

Figure 11. The changes of FMR (a), resonance frequency (c), and Q-factor are recorded. (b) is the derivative spectrum taken from (a) mathematically.

The excitation power of VNA is only tens dBm, and it is unlikely to drive the sample into non-linear regime. Signal intensity is proportional to $\sqrt{P}$ as indicated by eq. (6), however, SNR is found to be not much different if P is bigger than -20 dBm as demonstrated in Fig.12.

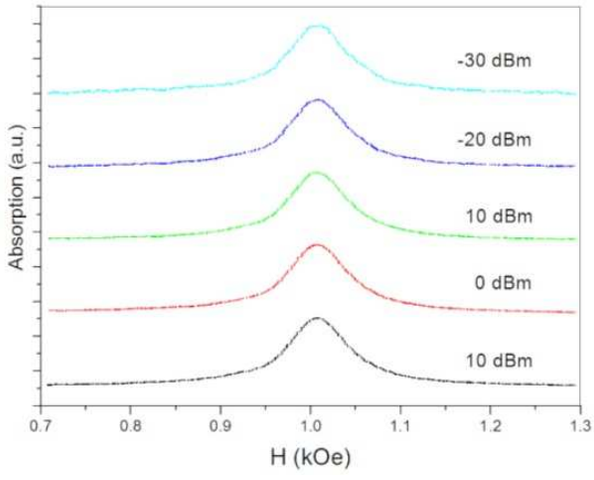

Figure 12. FMR signal of 10nm Py was recorded as function of excitation power. Note that these spectra have the same scale, but different offset for clear comparison.

As mentioned previously that VNA has very high frequency resolution, apparently, Q could be tuned as high as 140,000 and more by simply adjusting the iris. However, distorted spectrum is resulted at very high Q, and two peaks appear while Q is adjusted close to maximum Q as seen in Fig.13(a) and (b), respectively. It is also found that the SNR does not varied significantly if Q lies between 2,000 to 13,000 (the unloaded Q is about 9,000 as claimed). Surely, this finding is just for referral, and would depend very much on cavity used.

The advantages of the VNA-FMR with high Q cavity are: (1) the sensitivity which is comparable to that of commercials, but a lot cheaper, (2) multi frequencies can be done in

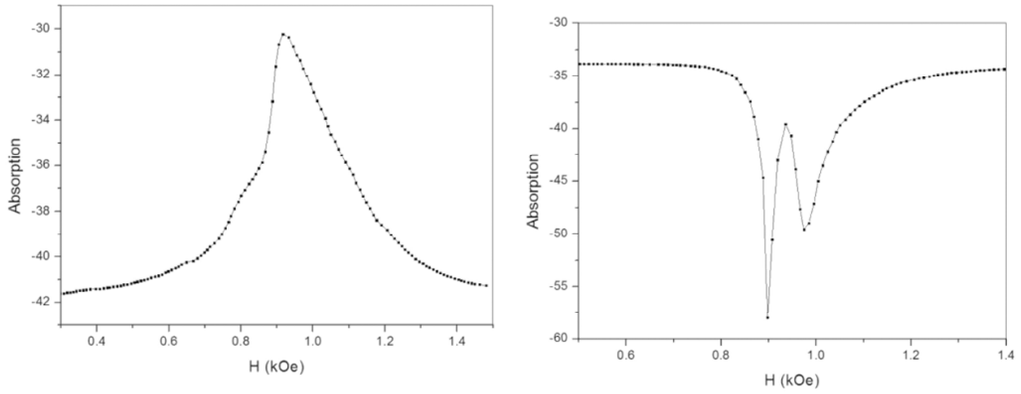

Figure 13. (a) data taken at Q ≈ 50,000, and (b) at ~110,000. Clearly, distorted signals are obtained.

the same manner by just changing to another band cavity only within the frequency range of the VNA. Nevertheless, some points needed to be well aware. Firstly, VNA has built-in sweep average function which increases the SNR for every sweeping. The penalty of using high average count is the very long acquisition time. For example, a commercial FMR spectrometer takes about a few seconds to sweep a spectrum over 2 kOe field at 1 Oe resolution with time constant of a 1mS. However, the settled time for a VNA with average of 1 is found to be about 0.1S a point. Therefore, it takes at least 3 min to obtain the spectrum with the same conditions. Average of 10, and sometime 50 are often used for better SNR, then the acquisition time is very long which could overheat the electromagnet. Secondary, VNA cannot work with lock-in amplifier directly, and a circulator is also needed to force the reflected wave to a new port. Before the signal is conducted to the lock-in amplifier, a microwave transducer (Schottky diode, for example) is required. This is because the output from VNA is power which has to be transduced into voltage before plugging into the lock-in amplifier. Besides, the output of VNA has already been averaged over a range of frequencies. Thus the Schottky detector cannot recognize this tiny average change. This problem can be amended by narrowing the starting and ending frequencies of the VNA. The two frequencies indeed can be set to the same value as the dip frequency. While working with lock-in, the VNA-FMR acquires data as fast as the commercial one, since the SNR enhancement is processed by the lock-in and not by the VNA. Further, MS-, and CPW- FMR can also work together with lock-in method in this manner. If one wants to study high power VNA-FMR, a high power microwave amplifier could be used. However, if the VNA is still used as the analyzer, a suitable attenuator has to be inserted between the returned line and VNA, otherwise damage is resulted.

Author details

Chi-Kuen Lo
Department of Physics, National Taiwan Normal University, Taipei, Taiwan

5. References

[1] M. Dı´az de Sihues, C. A. Durante-Rincon, and J. R. Fermin, J. Magn. Magn. Mater. 316, e462 (2007).

[2] V. G. Gavriljuk, A. Dobrinsky, B. D. Shanina, and S. P. Kolesnik, J. Phys. Condens. Matter 18, 7613 (2006).

[3] Z. Zhang, L. Zhou, P. E. Wigen, and K. Ounadjela, Phys. Rev. B 50(9), 6094 (1994).

[4] B. Heinrich, Y. Tserkovnyak, G. Woltersdorf, A. Brataas, R. Urban, and G. E. W. Bauer, Phys. Rev. Lett. 90(18), 187601 (2003).

[5] V. P. Nascimento and E. Baggio Saitovitch, F. Pelegrinia, L. C. Figueiredo, A. Biondo, and E. C. Passamani, J. Appl. Phys. 99, 08C108 (2006).

[6] K. Lenz, E. Kosubek, T. Tolinski, J. Lindner, and K. Baberschke, J. Phys.: Condens. Matter 15, 7175 (2003).

[7] M. Oogane, T. Wakitani, S. Yakata, R. Yilgin, Y. Ando, A. Sakuma, T. Miyazaki, J. J. Appl. Phys. 50 (5A) 3889 (2006)

[8] R. Urban, G. Woltersdorf, and B. Heinrich, Phys. Rev. Lett. 87(21), 271204-1 (2009).

[9] T. Kato, K. Nakazawa, R. Komiya, N. Nishizawa, S. Tsunashima, and S. Iwata, IEEE Trans. Magn., VOL. 44, NO. 11, NOVEMBER 2008

[10] "Microwave Electronics: Measurement and Materials Characterization", L. F. Chen, C. K. Ong, C. P. Neo, John Wileys & Sons Ltd. 2004

[11] "Microwave Engineering", D.M. Pozar, John Wileys & Sons Ltd. (2012)

[12] "High-Frequency EPR Instrumentation", E.J. Reijerse, Appl Magn Reson (2010) 37:795–818

[13] See http://www.bruker-biospin.com/epr-products.html.

[14] See http://www.jeol.com/PRODUCTS/AnalyticalInstruments/Electron SpinResonance/tabid/98/Default.aspx.

[15] "*Quantitative EPR"*, G. R. Eaton, S. S. Eaton, D. P. Barr, and R. T. Weber, Springer Wien, New York, (2010)

[16] Marina Vroubel, Yan Zhuang, Behzad Rejaei, and Joachim N. Burghartz, J. Appl. Phys. 99, 08P506 (2006)

[17] C. Nistor, K. Sun, Z. Wang, M. Wu, C. Mathieu, and Matthew Hadley Appl. Phys. Lett. 95, 012504 (2009)

[18] Y. Chen, D.S. Hung, Y.D. Yao, S.F. Lee, H.O. Ji, C. Yu, J. Appl. Phys. 101, 09C104 (2007)

[19] H. G LOWI'NSKI, J. DUBOWIK, Acta Physicae Superficierum , Vol. XII, 2012

[20] "The Art of Electronics", P. Horowitz, W. Hill, Cambridge Univ. Press, 2nd Ed. 1989

[21] Advanced Digital Signal Processing and Noise Reduction", S.V. Vaseghi, John Wiley & Sons Ltd., 2008

[22] Agilent VNA user manual

[23] C.K. Lo, W.C. Lai, J.C. Cheng, Rev. Sci. Instruments, 82, 086114 (2011)

[24] R.W. Damon, Rev. Mod. Phys., 25, No.1, 239 (1953)

[25] N. Bloembergen, S. Wang, Phys. Rev., 93 No.1 72 (1953)